Climatic Change (2019) 152:583–593
https://doi.org/10.1007/s10584-018-2348-2

Mortality risk from heat stress expected to hit poorest nations the hardest

Ali Ahmadalipour[1] · Hamid Moradkhani[1] · Mukesh Kumar[1]

Received: 24 August 2018 / Accepted: 3 December 2018 / Published online: 12 January 2019

Abstract

Anthropogenic climate warming has increased the likelihood of extreme hot summers. To facilitate mitigation and adaptation planning, it is essential to quantify and synthesize climate change impacts and characterize the associated uncertainties. By synergistically using projections of climate scenarios from an ensemble of regional climate models and a spatially explicit version of an empirical health risk model, here we quantify the mortality risk associated with excessive heat stress for people aged over 65 years old across the Middle East and North Africa (MENA). Our results show that mortality risk is expected to intensify by a factor of 8–20 in the last 30 years of the twenty-first century with respect to the historical period (1951–2005) if no climate change mitigation planning is undertaken. If global warming is limited to 2 °C, the mortality risk is expected to rise by a factor of 3–7 for the same period. Further analyses reveal that much of the increase in mortality risk is due to the increase in frequency of warm days rather than their intensity. Unfortunately, the poorest countries with least contribution to climate change are expected to be most impacted by it, as they will experience higher mortality risks compared to wealthier nations.

Key points

- A spatially explicit health risk model that accounts for regional temperature thresholds is utilized to quantify mortality risk in MENA.
- Substantial increase in mortality risk is expected, which is due to the increase in frequency of warm days rather than their intensity.
- Mortality risk ratio is found highest in poor nations with least contribution to anthropogenic climate change.

Electronic supplementary material The online version of this article (https://doi.org/10.1007/s10584-018-2348-2) contains supplementary material, which is available to authorized users.

✉ Ali Ahmadalipour
aahmada@ua.edu

Hamid Moradkhani
hmoradkhani@ua.edu

Mukesh Kumar
mkumar4@ua.edu

[1] Center for Complex Hydrosystems Research, Department of Civil, Construction, and Environmental Engineering, University of Alabama, Tuscaloosa, AL, USA

1 Introduction

Climate change will substantially affect human and biological systems, and it is likely to alter the boundaries of climate variability beyond historical observations (Li et al. 2018; McDowell et al. 2016; Nangombe et al. 2018). Frequent heat waves and escalating temperature and humidity have exacerbated heat stress (Guo et al. 2016; Li et al. 2017), with conditions in some cases exceeding the postulated thresholds of human tolerance (Zhao et al. 2016; Im et al. 2018), thus impairing health of millions of people (Honda et al. 2014; Pal and Eltahir 2016; Sylla et al. 2018a).

Deadly heat waves have struck many parts of the globe causing widespread economic losses (Burke et al. 2015, 2018), reduction in crop yield (Deryng et al. 2014), tree mortality (Liu et al. 2017), water and energy shortages (Lubega and Stillwell 2018; Tarroja et al. 2018), and—perhaps most concerning of all—impaired human health and mortality (Harrington et al. 2016; Mitchell 2016). High mortality caused by 2003 European heat waves garnered extensive societal attention (Christidis et al. 2015; Li et al. 2016b). Since then, several other heat wave events, including those in Russia in 2010 (Dole et al. 2011), Texas in 2011 (Luo and Zhang 2012), Australia in 2013 (Lewis and Karoly 2013), and eastern China (Sun et al. 2014; Miao et al. 2016b), Egypt (Mitchell 2016) and Europe (Kam et al. 2016) in 2015, have caused considerable mortality and morbidity. Notably, the likelihood of these extreme events has increased due to anthropogenic climate change (Ahmadalipour et al. 2017; Papalexiou et al. 2018; Sylla et al. 2018b). Given that the concentration of greenhouse gases (GHGs) is rising, heat stress morbidity and mortality are projected to increase in future (Lee and Kim 2016; Coffel et al. 2017).

Heat dissipation from the human body is aided through sweating and increased heart rate which helps raise the blood flow to the body surface thus facilitating thermoregulation. However, this may reduce the oxygen supply to muscles and brain (Checchi and Robinson 2013; Ghumman and Horney 2016; Huber et al. 2017), leading to mental and physical fatigue and subsequently increasing the likelihood of cardiovascular and respiratory diseases and mortality (Loughnan et al. 2010; Kjellstrom et al. 2016; Ross et al. 2018). Notably, the temperature that human body feels is different from the dry-bulb temperature (simply referred to as air temperature) (Willett and Sherwood 2012; Knutson and Ploshay 2016; Ross et al. 2018). The real-feel temperature is affected by humidity, radiation, wind speed, and cloud cover (depending on the season and study area) (Willett and Sherwood 2012; Dunne et al. 2013; Knutson and Ploshay 2016).

Although several prior works have examined the relation between air temperature extremes and mortality rate, i.e., number of fatality, at regional and local levels (Huber et al. 2017; Im et al. 2017; Mazdiyasni et al. 2017), such a study over the Middle East and North Africa—a region predominantly characterized by hot and arid climate and already intolerable for human beings in many parts—where climate warming is strongest in summer (Lelieveld et al. 2016; Russo et al. 2016) is sorely lacking.

Here we utilize a large ensemble of regional climate models to calculate spatially explicit wet-bulb temperature, which is then used within a recently developed health risk model to quantify mortality risk of people aged over 65 years old across the Middle East and North Africa (MENA). The regional climate models provide fine spatial resolution projections of climatological conditions under different future emission scenarios, while considering the regional characteristics of the climate system. Consideration of the ensemble results allows reliable characterization of uncertainty in mortality risk projections (Ahmadalipour et al. 2018).

The mortality risk in the health risk model is quantified based on the deviation from optimum temperature (the temperature at which the mortality risk is minimum) and the frequency of unsafe days. Instead of considering a constant unsafe temperature threshold, which cannot account for the regional tolerance to heat, a spatially explicit regional optimum temperature threshold is evaluated. It is to be noted that we limit our analyses to evaluation of mortality *risk*. This does not capture projections of human deaths per se since the extent of human mortality is substantially influenced by factors other than heat stress such as socioeconomic vulnerabilities, which can include air conditioning facilities, primary occupation (field vs. indoor), population, age, regional weather forecast accuracy and outreach, and medical infrastructure (Gasparrini et al. 2015; Mora et al. 2017). A preliminary health risk assessment of MENA region has been recently provided by Ahmadalipour and Moradkhani (2018a), which mainly focused on the ensemble mean of climate models. The current study is built upon the previous assessments and conducts a more detailed analysis to characterize the model and scenario uncertainties, investigate the role of frequency and intensity of heat stress on mortality risk, and reveal the correspondence between mortality risk and economic status of the affected regions. Probabilistic measures are employed to also assess the onset of mortality risk.

2 Materials and methods

2.1 Study area

The study area ranging from −6.6° S to 42.24° N latitude and −24.64° W to 60.28° E longitude is selected for analyses. Meteorological forcing at a daily temporal resolution and a spatial resolution of 0.44° is available for this area from the aforementioned 17 RCMs. The area covers parts of over 60 countries, accommodating more than 600 million inhabitants (Dosio 2016; Lelieveld et al. 2016). Climate of the region is mostly characterized by hot arid areas with very low precipitation (Lelieveld et al. 2012, 2016; Waha et al. 2017). The Sahara Desert in northern Africa and parts of the Middle East are among the driest regions in the globe (Ahmadalipour and Moradkhani 2018b). Notably, the study region consists of very humid regions too. This is important, especially as humidity variations may have substantial effects on the real-feel temperature as well.

2.2 Climate data

Maximum near surface air temperature (*Tx*) and relative humidity (*hurs*) are acquired at a daily temporal resolution for summer months (June, July, and August) from meteorological data repository developed by the Coordinated Regional Climate Downscaling Experiment (CORDEX) (Jones et al. 2011). Here, we considered data from 17 regional climate models (RCMs) for a historical period ranging from 1951 to 2005 and three future periods viz., near future (2010–2039), intermediate future (2040–2069), and distant future (2070–2099). Two GHG representative concentration pathways viz., RCP4.5 corresponding to 2 °C global warming by the end of twenty-first century and RCP8.5 corresponding to "business as usual" pathway, are considered for each RCM. Previous studies have evaluated CORDEX RCMs in terms of their ability to capture *Tx* and *hurs* and found reasonable performance for most regions (Önol et al. 2013; Kim et al. 2014; Diasso and Abiodun 2017; Nikiema et al. 2017; Ring et al. 2017). In general, intrinsic biases are inevitable in climate models due to epistemic

uncertainties and model parameterizations (Miao et al. 2016a; Rocheta et al. 2017). Although not performed here, the application of bias correction methods is expected to improve the reliability of climate projections (Nahar et al. 2018; Nguyen et al. 2018). Among the methods developed for bias correction, the multivariate bias correction tools are capable of enhancing the joint dependence of variables, which is beneficial in multitude of applications (Mehrotra et al. 2018). More information about the RCMs and their characteristics can be found in Supplementary Table S1.

2.3 GDP and emission data

Gross domestic product (GDP) per capita and total greenhouse gas emissions data are acquired from the World Bank for 2010 (World Bank 2010). The year 2010 was chosen to ensure data availability for all studied countries.

The methodology employed in this study is thoroughly explained in Ahmadalipour and Moradkhani (2018a). To ensure accessibility for all the readers, an overview of the methodology is provided in the Supplementary Information (SI) section 1.

3 Results and discussion

Mortality risk ratio (MRR, see SI section 1.3), which indicates the relative risk of a 30 year future period with respect to the historical period (1951–2005), is obtained (Fig. 1). The evaluation is performed using data from each of the 17 RCMs for two future GHG emission scenarios (i.e., RCP4.5 and RCP8.5). Figure 1 shows both regional and latitudinal exacerbations of mortality risk compared to the historical period. Results also indicate minimal difference between the two emission scenarios in the near future period (i.e., 2010–2039), with both scenarios indicating risk ratios ranging between 1 and 5 and low model uncertainty (relatively low coefficient of variation, as shown in Supplementary Figure S8). However, the disparity between the two future scenarios rises in the distant future period (i.e., 2070–2099), yielding mortality risk ratios higher than 30 in some regions for RCP8.5. For the latitudinal mean mortality risk ratio, a similar pattern is found in all the three selected future periods and scenarios, with central African countries located around 12° N exhibiting the highest risk ratio (and the highest uncertainty) and northern African countries around 21° N showing the lowest ratio.

In the following context, model uncertainty is the range of projections from various models for a particular scenario, and scenario uncertainty is the difference of the projections from various RCPs. Numerous methods have been developed in recent years to properly quantify the uncertainties of climate projections (Najafi and Moradkhani 2015; Li et al. 2016a; Woldemeskel et al. 2016). Here, the standard deviation of projections (the 2nd and 4th columns in Fig. 1) provides a measure of model uncertainty, and the difference between the ensemble mean of the two RCPs indicates the scenario uncertainty. The last column of Fig. 1 reveals the uncertainties at different latitudes, where model uncertainty can be identified by the spread of the shaded area, and scenario uncertainty is the difference between the red and blue lines. As it can be seen, the shaded areas have larger overlap in the near future, and the ensemble mean lines are in close proximity, whereas in the distant future, the projections of the two RCPs have almost no overlap, indicating a considerably higher scenario uncertainty in the distant future. In summary, model uncertainty is found to be the major source of uncertainty in

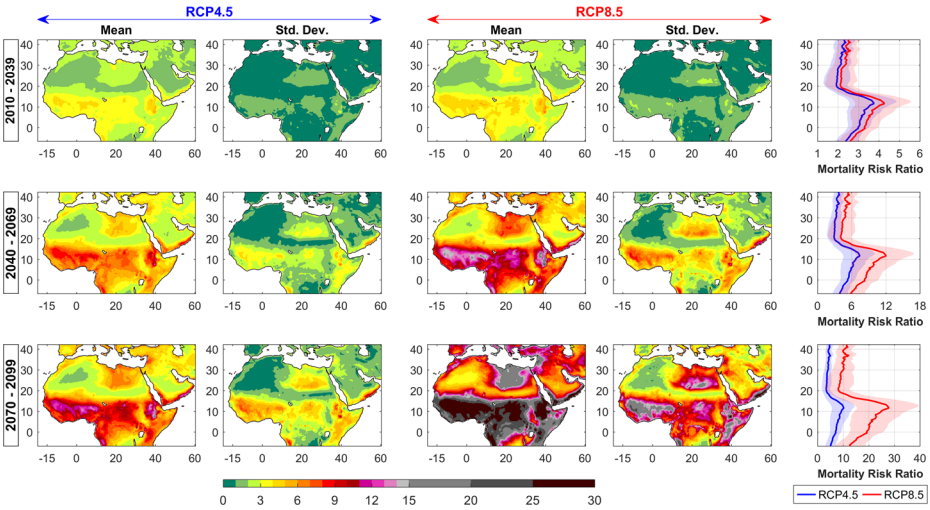

Fig. 1 Ensemble mean and standard deviation (calculated from 17 RCMs) of mortality risk ratio. The shaded plots in the rightmost column represent mean ± 1 standard deviation of mortality risk ratio. Mortality risk ratio indicates the ratio of mortality risk in a future period compared to that for the historical period. A similar latitudinal pattern is found for all periods and scenarios with higher uncertainty for RCP8.5

the near future (2010–2039), whereas scenario uncertainty is the major contributor in the distant future (2070–2099). It is to be noted that if bias corrected models were applied, the regional model uncertainty would have been different, but the overall pattern would have been somewhat similar, and the scenario uncertainty is inevitably large in the distant future.

In order to better understand the role of intensity of unsafe temperatures (ΔTW) and percentage of unsafe days, the mortality risk ratio in each future period is plotted against the two influencing components for the entire ensemble of models. Figure 2 shows the distribution of each component and the corresponding mortality risk ratio acquired from the entire grids and models. The figure shows that at any particular frequency of unsafe days, the mortality risk ratio is almost the same for different ΔTW, i.e., the scatterplot color does not change vertically. Therefore, the influence of the frequency of unsafe days on mortality risk is found to be higher than ΔTW, especially in the distant future period. The presented results are also true for the ten largest cities in MENA (see SI section 4). Furthermore, climate change will substantially increase the number of unsafe days while also altering the bell-shaped (with a bit of positive skewness) distribution of frequency of unsafe days from positively skewed to a negatively skewed distribution.

In order to better clarify the role of each factor on mortality risk, two hypothetical cases are considered, both of which fall within the feasible range of variations:

- Case A: 20 unsafe days with dT = 1.5 °C (on average)
- Case B: 60 unsafe days with dT = 1 °C (on average)

The Summer Excess Mortality Risk (SI section 1.3) for cases A and B are calculated as 0.23 and 0.41, respectively. Therefore, although the intensity of heat stress in case A is 0.5 °C (50%) higher than case B, the excess mortality risk of case B is about twice that of case A.

The cumulative distribution function (CDF) of ΔTW through time shows rightward shift for both low and high percentiles (Fig. 3). In contrast, CDF of frequency of unsafe days

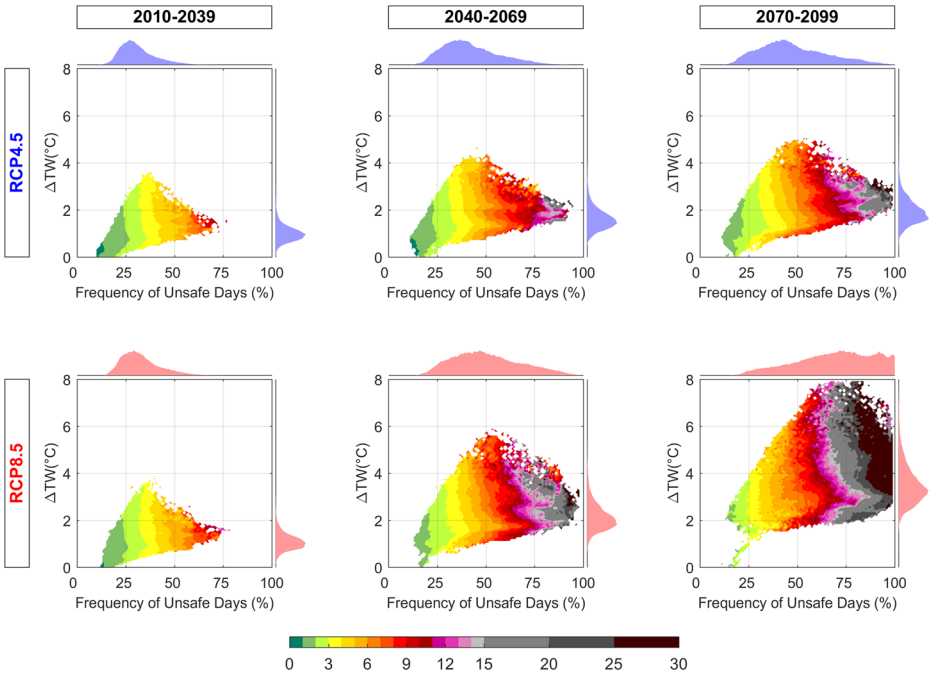

Fig. 2 Density-type scatterplots comparing ΔTW (on *y*-axis), frequency (percentage) of unsafe days (on *x*-axis), and mortality risk ratio (colorbar) for each period and each scenario. For each case, the probability distribution of ΔTW and frequency of unsafe days are shown besides their corresponding axes. Each plot is generated using about 230,000 values (17 models × 13,527 grids)

indicate changes in its distribution, with rightward shift for high percentiles and minor changes at the low percentiles. This change of distribution results in substantial increase in the median value of percentage of unsafe days from 30% in the near future period to 45% and 70% in the distant future for RCP4.5 and RCP8.5, respectively. The consequence is a significant shift in distribution of mortality risk ratio, particularly at high percentiles. Moreover, the difference between the two future scenarios is more pronounced in the distant future period, with the median of mortality risk ratio for RCP8.5 (MRR ≈ 12) being almost equal to the 95th percentile of RCP4.5. In other words, in the distant future (2070–2099), the most likely (median) mortality risk ratio in the business as usual emission scenario (i.e., RCP8.5) is expected to exceed the least likely (95th percentile) risk levels of RCP4.5 scenario.

Spatial variation of mortality risk ratio over the study area showed highest risk ratios in central Africa and the regions below the Sahara desert. As economic factors, which govern access to forecasts of extremes and air conditioning and healthcare facilities, can play a critical role in translation of heat stress-induced mortality risk into actual mortality occurrence, we investigate the correspondence between mortality risk ratio and economic status of the affected regions. To facilitate the analysis, 56 countries in the study region are classified into four quartiles according to their GDP (gross domestic product) per capita values. Figure 4 shows the distribution of mortality risk ratio in the distant future period for RCP8.5. The figure (plot A) illustrates that the wealthy countries (high GDP per capita in 4th quartile) are expected to experience considerably lower mortality risk ratios compared to the poorest nations. This is notwithstanding the fact that the wealthy countries have much higher contribution in causing

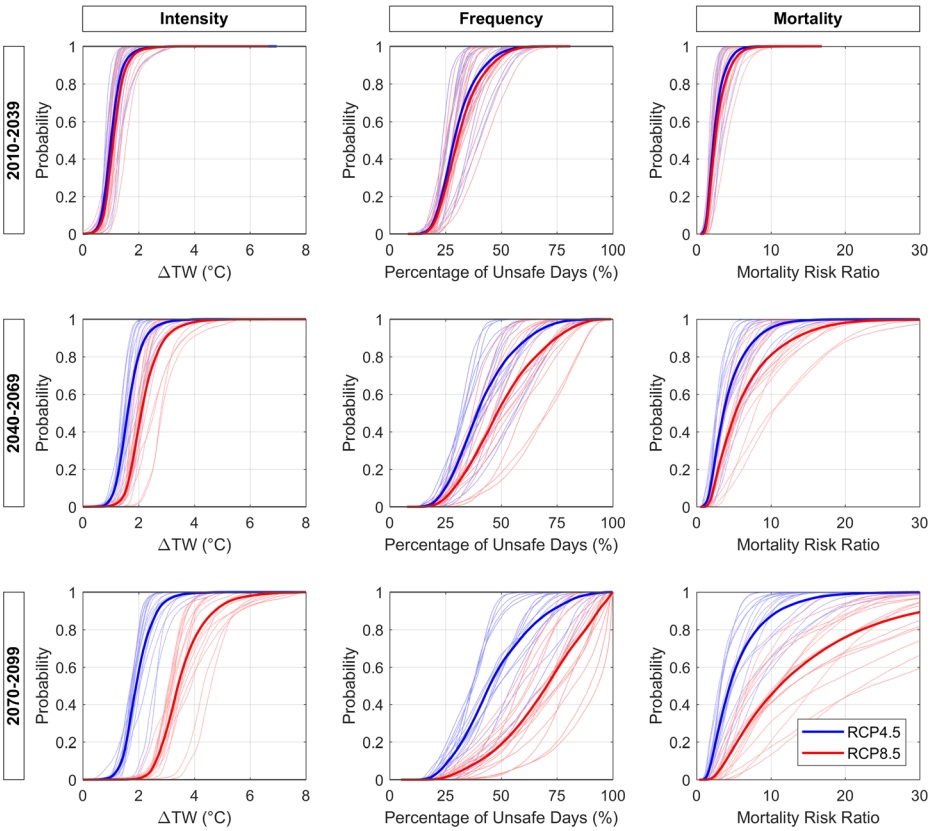

Fig. 3 Cumulative density function (CDF) of intensity (ΔTW, shown in the left column), frequency (shown in the middle column), and mortality risk ratio (shown in the right column). Each plot is generated using data for the entire MENA region. Each CDF line indicates result of an RCM, and the bold lines in the middle represent the multi-model mean. A shift to the right in CDF plot implies an increase in the variable of interest. From the figure, in the distant future period, the median (most likely) mortality risk ratio of RCP8.5 is almost the same as the 95th percentile (least likely) risk of RCP4.5 projections

anthropogenic climate change by generating significantly higher greenhouse gas emissions (plots B and C). The inequality of climate change impacts has drawn more attention in recent years, and it has been shown that global warming hits poorest countries hardest (Burke et al. 2015; Harrington et al. 2016; King and Harrington 2018). Our result adds to this narrative and shows that climate change impacts on heat stress are expected to also weigh down the poorer countries much more. The analyses explicate the urgency for mitigating climate change in order to ameliorate social and health-related risks of a warmer world in future. Unlike developed and wealthy countries with ubiquitous and public access to air conditioning facilities, advanced medical centers, and established national/local weather forecast centers with extensive outreach and early warning systems, poorer nations are significantly more vulnerable to heat stress (Mora et al. 2017; Ahmadalipour and Moradkhani 2018b). For instance Benin, a country in western Africa with low GDP per capita and poor infrastructure, is projected to experience the highest mortality risk ratio among the 56 countries in the Middle East and North Africa. Unfortunately, the country has only 41% of its population with access to electricity, and this rate is reduced to 18% for the rural population (World Bank 2010).

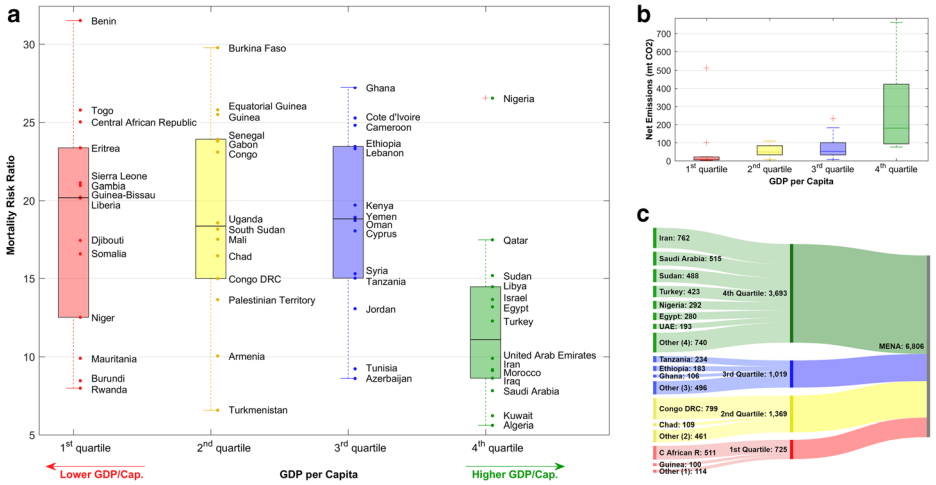

Fig. 4 **a** Distribution of mortality risk ratio among the 56 studied countries in the MENA region, divided into four quartiles based on their GDP per capita. The line in the middle of each box represents the median mortality risk ratio in each case. **b** The amount of net emissions of greenhouse gases (megaton equivalent of CO_2) as of 2010 corresponding to each GDP per capita quartile. **c** Flowchart of the total greenhouse gas emissions (million tons of CO_2 emitted in 2010) classified for GDP quartiles and the major contributing countries in each quartile. The figure shows that the poorest nations (in the 1st quartile) generate the least emissions but will experience the highest mortality risk ratio, whereas wealthy countries generate the highest emissions and will be least impacted by climate change (based on mortality risk ratio). The results of RCP4.5 scenario (see Supplementary Figure S4) show similar patterns.

Hence, access to air conditioning facilities is not an option for the majority of people in Benin. Notably, although the contribution of the 1st quartile (poorest) countries to the total greenhouse gas emissions is on order of magnitude less than that of the 4th quartile (richest) countries, the impacts of climate change will hit the poorer nations the hardest. It is to be noted that such a conclusion is based on the overall pattern of the quartiles. Some countries do fall outside of this broad-brush conclusion. For instance, the MRR for Rwanda (with low GDP/cap.) is less than the majority of 1st quartile countries. Overall, the poorest (1st quartile) and wealthiest (4th quartile) countries exhibit highest and lowest MRR, respectively.

4 Concluding remarks

This study provided an interdisciplinary and probabilistic assessment of heat stress mortality risk of people aged over 65 years old across the Middle East and North Africa (MENA) and investigated the impacts of climate change on it. The results revealed the inequality of climate change impacts on poor versus wealthy nations and pointed out the necessity of climate change mitigation and reducing net emissions for attenuating deleterious future risks of excessive heat on human morbidity and mortality (Harrington et al. 2016; Pal and Eltahir 2016; Mora et al. 2017). Furthermore, we found that mortality risk will be significantly lower if global air temperature rise is limited to 2 °C (i.e., RCP4.5). Recent analyses emphasize that it is still possible to reach the Paris agreement goals and limit global warming below 2 °C by 2100 (Millar et al. 2017). The sooner countries commit to reducing net emissions and work upon stabilizing climate, the higher is the likelihood of mitigating the impacts of climate change on mortality risk (Li et al. 2017; Nangombe et al. 2018).

Acknowledgements We would like to acknowledge the Coordinated Regional Climate Downscaling Experiment (CORDEX) for providing access to climate models. We also appreciate the World Bank for providing data for greenhouse gases emissions and GDP per capita at national level.

Compliance with ethical standards

Conflict of interest The authors declare that they have no conflict of interest.

Publisher's Note Springer Nature remains neutral with regard to jurisdictional claims in published maps and institutional affiliations.

References

Ahmadalipour A, Moradkhani H (2018a) Escalating heat-stress mortality risk due to global warming in the Middle East and North Africa (MENA). Environ Int 117:215–225. https://doi.org/10.1016/j.envint.2018.05.014

Ahmadalipour A, Moradkhani H (2018b) Multi-dimensional assessment of drought vulnerability in Africa: 1960–2100. Sci Total Environ 644:520–535. https://doi.org/10.1016/j.scitotenv.2018.07.023

Ahmadalipour A, Moradkhani H, Svoboda M (2017) Centennial drought outlook over the CONUS using NASA-NEX downscaled climate ensemble. Int J Climatol 37:2477–2491. https://doi.org/10.1002/joc.4859

Ahmadalipour A, Moradkhani H, Rana A (2018) Accounting for downscaling and model uncertainty in fine-resolution seasonal climate projections over the Columbia River Basin. Clim Dyn 50:717–733. https://doi.org/10.1007/s00382-017-3639-4

Burke M, Hsiang SM, Miguel E (2015) Global non-linear effect of temperature on economic production. Nature 527:235–239

Burke M, Davis WM, Diffenbaugh NS (2018) Large potential reduction in economic damages under UN mitigation targets. Nature 557:549

Checchi F, Robinson WC (2013) Mortality among populations of southern and central Somalia affected by severe food insecurity and famine during 2010–2012. Food and Agriculture Organization of the United Nations, Rome

Christidis N, Jones GS, Stott PA (2015) Dramatically increasing chance of extremely hot summers since the 2003 European heatwave. Nat Clim Chang 5:46–50

Coffel ED, Horton RM, de Sherbinin A (2017) Temperature and humidity based projections of a rapid rise in global heat stress exposure during the 21st century. Environ Res Lett 13:14001

Deryng D, Conway D, Ramankutty N et al (2014) Global crop yield response to extreme heat stress under multiple climate change futures. Environ Res Lett 9:34011

Diasso U, Abiodun BJ (2017) Drought modes in West Africa and how well CORDEX RCMs simulate them. Theor Appl Climatol 128:223–240

Dole R, Hoerling M, Perlwitz J et al (2011) Was there a basis for anticipating the 2010 Russian heat wave? Geophys Res Lett. https://doi.org/10.1029/2010GL04658

Dosio A (2017) Projection of temperature and heat waves for Africa with an ensemble of CORDEX regional climate models. Clim Dyn 49(1-2):493–519

Dunne JP, Stouffer RJ, John JG (2013) Reductions in labour capacity from heat stress under climate warming. Nat Clim Chang 3:563–566

Gasparrini A, Guo Y, Hashizume M et al (2015) Temporal variation in heat–mortality associations: a multicountry study. Environ Health Perspect 123:1200

Ghumman U, Horney J (2016) Characterizing the impact of extreme heat on mortality, Karachi, Pakistan, June 2015. Prehosp Disaster Med 31:263–266

Guo Y, Li S, Li Liu D et al (2016) Projecting future temperature-related mortality in three largest Australian cities. Environ Pollut 208:66–73

Harrington LJ, Frame DJ, Fischer EM et al (2016) Poorest countries experience earlier anthropogenic emergence of daily temperature extremes. Environ Res Lett 11:55007

Honda Y, Kondo M, McGregor G et al (2014) Heat-related mortality risk model for climate change impact projection. Environ Health Prev Med 19:56–63

Huber V, Ibarreta D, Frieler K (2017) Cold-and heat-related mortality: a cautionary note on current damage functions with net benefits from climate change. Clim Chang 142(3-4):407–418
Im E-S, Pal JS, Eltahir EAB (2017) Deadly heat waves projected in the densely populated agricultural regions of South Asia. Sci Adv 3:e1603322
Im E-S, Kang S, Eltahir EAB (2018) Projections of rising heat stress over the western Maritime Continent from dynamically downscaled climate simulations. Glob Planet Change 165:160–172
Jones C, Giorgi F, Asrar G (2011) The Coordinated Regional Downscaling Experiment: CORDEX–an international downscaling link to CMIP5. CLIVAR Exch 56:34–40
Kam J, Knutson TR, Zeng F, Wittenberg AT (2016) Multimodel assessment of anthropogenic influence on record global and regional warmth during 2015. Bull Am Meteorol Soc 97:S4–S8
Kim J, Waliser DE, Mattmann CA et al (2014) Evaluation of the CORDEX-Africa multi-RCM hindcast: systematic model errors. Clim Dyn 42:1189–1202
King AD, Harrington LJ (2018) The inequality of climate change from 1.5°C to 2°C of global warming. Geophys Res Lett 45:5030–5033
Kjellstrom T, Briggs D, Freyberg C et al (2016) Heat, human performance, and occupational health: a key issue for the assessment of global climate change impacts. Annu Rev Public Health 37:97–112
Knutson TR, Ploshay JJ (2016) Detection of anthropogenic influence on a summertime heat stress index. Clim Chang 138:25–39
Lee JY, Kim H (2016) Projection of future temperature-related mortality due to climate and demographic changes. Environ Int 94:489–494
Lelieveld J, Hadjinicolaou P, Kostopoulou E et al (2012) Climate change and impacts in the Eastern Mediterranean and the Middle East. Clim Chang 114:667–687. https://doi.org/10.1007/s10584-012-0418-4
Lelieveld J, Proestos Y, Hadjinicolaou P et al (2016) Strongly increasing heat extremes in the Middle East and North Africa (MENA) in the 21st century. Clim Chang 137:245–260
Lewis SC, Karoly DJ (2013) Anthropogenic contributions to Australia's record summer temperatures of 2013. Geophys Res Lett 40:3705–3709
Li J, Sharma A, Evans J, Johnson F (2016a) Addressing the mischaracterization of extreme rainfall in regional climate model simulations—a synoptic pattern based bias correction approach. J Hydrol 556:901–912
Li T, Horton RM, Bader DA et al (2016b) Aging will amplify the heat-related mortality risk under a changing climate: projection for the elderly in Beijing, China. Sci Rep 6:28161
Li C, Zhang X, Zwiers F, et al (2017) Recent very hot summers in northern hemispheric land areas measured by wet bulb globe temperature will be the norm within 20 years. Earth's Futur
Li C, Fang Y, Caldeira K et al (2018) Widespread persistent changes to temperature extremes occurred earlier than predicted. Sci Rep 8:1007
Liu Y, Parolari AJ, Kumar M et al (2017) Increasing atmospheric humidity and CO2 concentration alleviate forest mortality risk. Proc Natl Acad Sci 114:9918–9923
Loughnan M, Nicholls N, Tapper N (2010) Mortality–temperature thresholds for ten major population centres in rural Victoria, Australia. Health Place 16:1287–1290
Lubega WN, Stillwell AS (2018) Maintaining electric grid reliability under hydrologic drought and heat wave conditions. Appl Energy 210:538–549
Luo L, Zhang Y (2012) Did we see the 2011 summer heat wave coming? Geophys Res Lett 39:L09708
Mazdiyasni O, AghaKouchak A, Davis SJ et al (2017) Increasing probability of mortality during Indian heat waves. Sci Adv 3:e1700066
McDowell NG, Williams AP, Xu C et al (2016) Multi-scale predictions of massive conifer mortality due to chronic temperature rise. Nat Clim Chang 6:295
Mehrotra R, Johnson F, Sharma A (2018) A software toolkit for correcting systematic biases in climate model simulations. Environ Model Softw 104:130–152
Miao C, Su L, Sun Q, Duan Q (2016a) A nonstationary bias-correction technique to remove bias in GCM simulations. J Geophys Res Atmos 121(10):5718–5735
Miao C, Sun Q, Kong D, Duan Q (2016b) Record-breaking heat in northwest China in July 2015: analysis of the severity and underlying causes. Bull Am Meteorol Soc 97:S97–S101
Millar RJ, Fuglestvedt JS, Friedlingstein P et al (2017) Emission budgets and pathways consistent with limiting warming to 1.5°C. Nat Geosci 10:741–747. https://doi.org/10.1038/ngeo3031
Mitchell D (2016) Human influences on heat-related health indicators during the 2015 Egyptian heat wave. Bull Am Meteorol Soc 97:S70–S74
Mora C, Dousset B, Caldwell IR et al (2017) Global risk of deadly heat. Nat Clim Chang 7:501–506
Nahar J, Johnson F, Sharma A (2018) Addressing spatial dependence bias in climate model simulations—an independent component analysis approach. Water Resour Res 54:827–841
Najafi MR, Moradkhani H (2015) Multi-model ensemble analysis of runoff extremes for climate change impact assessments. J Hydrol 525:352–361. https://doi.org/10.1016/j.jhydrol.2015.03.045

Nangombe S, Zhou T, Zhang W et al (2018) Record-breaking climate extremes in Africa under stabilized 1.5 °C and 2°C global warming scenarios. Nat Clim Chang 8:375–380. https://doi.org/10.1038/s41558-018-0145-6
Nguyen H, Mehrotra R, Sharma A (2018) Correcting systematic biases across multiple atmospheric variables in the frequency domain. Clim Dyn 1–16. https://doi.org/10.1007/s00382-018-4191-6
Nikiema PM, Sylla MB, Ogunjobi K et al (2017) Multi-model CMIP5 and CORDEX simulations of historical summer temperature and precipitation variabilities over West Africa. Int J Climatol 37:2438–2450
Önol B, Bozkurt D, Turuncoglu UU et al (2013) Evaluation of the twenty-first century RCM simulations driven by multiple GCMs over the Eastern Mediterranean–Black Sea region. Clim Dyn 42:1949–1965. https://doi.org/10.1007/s00382-013-1966-7
Pal JS, Eltahir EAB (2016) Future temperature in southwest Asia projected to exceed a threshold for human adaptability. Nat Clim Chang 6:197–200
Papalexiou SM, AghaKouchak A, Trenberth KE, Foufoula-Georgiou E (2018) Global, regional, and megacity trends in the highest temperature of the year: diagnostics and evidence for accelerating trends. Earth's Futur 6:71–79
Ring C, Pollinger F, Kaspar-Ott I et al (2017) A comparison of metrics for assessing state-of-the-art climate models and implications for probabilistic projections of climate change. Clim Dyn 50(5-6):2087–2106
Rocheta E, Evans JP, Sharma A (2017) Can bias correction of regional climate model lateral boundary conditions improve low-frequency rainfall variability? J Clim 30:9785–9806
Ross ME, Vicedo-Cabrera AM, Kopp RE et al (2018) Assessment of the combination of temperature and relative humidity on kidney stone presentations. Environ Res 162:97–105
Russo S, Marchese AF, Sillmann J, Immé G (2016) When will unusual heat waves become normal in a warming Africa? Environ Res Lett 11:54016
Sun Y, Zhang X, Zwiers FW et al (2014) Rapid increase in the risk of extreme summer heat in Eastern China. Nat Clim Chang 4:1082–1085
Sylla MB, Faye A, Giorgi F, et al (2018a) Projected heat stress under 1.5°C and 2°C global warming scenarios creates unprecedented discomfort for humans in West Africa. Earth's Futur 6(7):1029–1044
Sylla MB, Faye A, Klutse NAB, Dimobe K (2018b) Projected increased risk of water deficit over major West African river basins under future climates. Clim Change 151(2):247–258
Tarroja B, Chiang F, AghaKouchak A, Samuelsen S (2018) Assessing future water resource constraints on thermally based renewable energy resources in California. Appl Energy 226:49–60
Waha K, Krummenauer L, Adams S et al (2017) Climate change impacts in the Middle East and Northern Africa (MENA) region and their implications for vulnerable population groups. Reg Environ Chang 17:1623–1638
Willett KM, Sherwood S (2012) Exceedance of heat index thresholds for 15 regions under a warming climate using the wet-bulb globe temperature. Int J Climatol 32:161–177
Woldemeskel FM, Sharma A, Sivakumar B, Mehrotra R (2016) Quantification of precipitation and temperature uncertainties simulated by CMIP3 and CMIP5 models. J Geophys Res Atmos 121:3–17
World Bank (2010) GDP per capita (current US $). Retreived from https://data.worldbank.org/indicator/NY.GDP.PCAP.CD. Accessed 5 June 2018
Zhao Y, Sultan B, Vautard R et al (2016) Potential escalation of heat-related working costs with climate and socioeconomic changes in China. Proc Natl Acad Sci 113:4640–4645